TRANSIENT COMPUTATIONAL FLUID DYNAMICS INVESTIGATIONS ON THERMAL PERFORMANCE OF SOLAR AIR HEATER WITH HOLLOW VERTICAL FINS

by

Duraisamy JAGADEESH[a*], Ramasamy VENKATACHALAM[b], and Gurusamy NALLAKUMARASAMY[c]

[a] Department of Mechanical Engineering, Kongunadu College of Engineering and Technology, Tiruchirappalli, Tamil Nadu, India
[b] Department of Mechanical Engineering, KSR College of Engineering, Namakkal, Tamil Nadu, India
[c] Department of Mechanical Engineering, Excel Engineering College, Namakkal, Tamil Nadu, India

Original scientific paper
https://doi.org/10.2298/TSCI170531297D

Evaluation of experimental thermal performance of a single pass solar air dryer is compared with a transient CFD studies is performed. Vertical hollow plates are placed below the absorber plate and compared against the flat solar absorber plate for its performance improvement. Effect of mass-flow rate, the outlet temperature of air is computationally analyzed in comparison with the experimental work, transient boundary conditions for CFD like ambient temperature, solar insolation are taken from the experimental work, and computational results are in good agreement of with experimental results with maximum error percentage of 10%. Thermal efficiency was increased with increase in mass-flow area for without fin configuration, for a specific mass-flow rate thermal efficiency had a good improvement with fin configuration than the without fin configuration.

Key words: *CFD, fins, solar air heater, flow simulation*

Introduction

Solar air heaters are widely used in food industries to dry the agricultural products to make agricultural products a value addition, solar air dryer is used to harness solar insolation in which its performance can be enhanced by using fins below or above the absorber plates. In this paper, transient CFD is employed to study the performance of solar air heater with and without fin configuration, fins are made semi-cylindrical hollow shape and it is placed longitudinally below the absorber plates, solar air heater *works* as single pass system. Semi-cylindrical form is one of the novel *approach* for the fin design and this has been proposed to improve the thermal efficiency of the system. The evaluation of the results of experimental with CFD shows by enhancing the heat transfer area using fins will increase the rate of heat transfer of the fluid, but it is a tradeoff between pressure drop and enhanced heating surface area, by providing fins pressure drop increases with increased power to the blower [1, 2]. Many shapes and configurations of solar collector plates have been modeled to enhance the heat transfer coefficient. The various baffles and artificial hurdles were used to increase rate of heat transfer between absorber plate and working fluid which is air [3]. Analytical and experimental analysis was performed

* Corresponding author, e-mail: jagadeesh.kncet@gmail.com

in the cross-corrugated absorber plate for different configurations, cross-corrugated plate on the top, bottom and in zigzag position, cross-corrugated absorber plate significantly improves the thermal performance of the solar air heater [4]. A new device is tested numerically and experimentally with fins and baffle arrangement with double pass over the tube plate, this fin and baffle arrangement substantially improves the heat transfer efficiency [5]. Thermal performance done for the three types of air heaters, with fins and without fins below the absorber plate, the efficiency of finned collector is higher than the without fin collector [6]. Thermal performance was done on solar air heater double and single and double pass arrangement for two flow rates using meshed wire as absorber plate, bed height also modified for two configurations, results reveals increasing efficiency by increasing the flow rate, also efficiency of double is more than of single pass configuration, wire-meshed arranged in layers proves a substantial improvement in thermal efficiency than the conventional flat solar absorber plate [7]. Double pass finned solar air heater is investigated experimentally and numerically, fins on the absorber plates are of rods and corrugated, corrugated absorber plate is more efficient than the rod type fins, thermal efficiency increases with increase in the mass-flow rates [8]. Flow of fluid to be heated is improved when its send across bottom of the absorber plate, and it was less when its send across at the top of absorber plate, efficiency of all types of system tried goes up by increasing the mass-flow rate, porous type absorber plate has better efficiencies in comparison with non-porous type absorber plates [9]. Aluminum can has been used for manufacturing the absorber plate, it improves the collector efficiency and also increases the rate of heat transfer between absorber plate and fluid. As it utilizes the aluminum cans cost of solar heater will be very less and it improves the sustainability [10]. The CFD of solar air heater is performed as 2-D simulations and they have utilized novel hyperbolic as geometry for the ribs, performance studies are compared with rectangular, triangular, and semicircular ribs against the hyperbolic ribs, optimum performance is obtained for hyperbolic ribs [11]. The CFD analysis is performed for solar air heater, having rib in the form of inverted L shape, rib generates the vortices which will enhance the heat transfer rate between absorber and working fluid. Optimization is done to select the optimal size of L shape fin [12]. A CFD study was done to measure the performance of non-uniform and uniform transverse ribs, they have employed k-ε equation as turbulence model Nusselt number is higher for non-uniform transverse ribs [13-19]. The performance and outlet temperature of grooved type solar air heater and flat plate solar air heater at different mass-flow rates are studied and the analyzed result shows that the grooved heater is 14% more efficient than the flat type heaters at 35° atmospheric temperature and various mass-flow rates. The difference in outlet temperature varies up to 3 °C between the grooved type and the flat type heaters [20].

In a study [21], the numerical models of flat plate and v-corrugated plate solar heaters are developed. For these solar heaters experimental and theoretical analysis was done. The theoretical assumptions were matched with experimental data. The parameters which are taken for the comparison is outlet temperatures of air-flow, output power and overall heat losses of the two heaters. The consequences of pressure drop in air, efficiencies for these two heaters are also analyzed. The highest value of thermohydraulic efficiency was attained at the mass-flow rate of 0.02 kg/s. The use of corrugated type absorber plate is as good as flat plate absorber plate in the solar air heater.

The objective of this paper is to evaluate the experimental thermal performance of a single pass solar air dryer take from [14] and it is compared with a transient CFD studies using solid works flow simulation. Novelty of the work is to relate to solar air heater using fins and evaluating the same using CFD using conjugate heat transfer with transient boundary conditions.

Computational methods

Software used in this study is called Solid WorksFlow Simulation, it has advantage of the conventional CFD software, which allows the conjugate heat transfer without any complex methods for meshing and preparing shadows and interfaces for the fluid domain.

Governing equations – general

The conservation laws for mass, angular momentum and energy in the Cartesian co-ordinate system rotating with angular velocity, Ω, about an axis passing through the co-ordinate system's origin can be written in the conservation form:

$$\frac{\partial \rho}{\partial t} + \frac{\partial}{\partial x_i}\left(\rho u_i\right) = 0 \tag{1}$$

$$\frac{\partial \rho u_i}{\partial t} + \frac{\partial}{\partial x_i}\left(\rho u_i u_j\right) + \frac{\partial p}{\partial x_i} = \frac{\partial}{\partial x_j}\left(\boldsymbol{\tau}_{ij} + \boldsymbol{\tau}_{ij}^R\right) + S_i \quad i = 1,2,3 \tag{2}$$

$$\frac{\partial \rho H}{\partial t} + \frac{\partial \rho u_i H}{\partial x_i} = \frac{\partial}{\partial x_i}\left[u_j(\boldsymbol{\tau}_{ij} + \boldsymbol{\tau}_{ij}^R) + q_i\right] + \frac{\partial p}{\partial t} - \boldsymbol{\tau}_{ij}^R \frac{\partial u_i}{\partial x_j} + \rho\varepsilon + S_i u_i + Q_H \tag{3}$$

$$H = h + \frac{u^2}{2} \tag{4}$$

where u is the fluid velocity, ρ – the fluid density, S_i – the mass-distributed external force per unit mass due to: a porous media resistance (S_i^{porous}), a buoyancy ($S_i^{\text{gravity}} = -\rho g_i$, where g_i is the gravitational acceleration component along the i^{th} co-ordinate direction), and the co-ordinate system's rotation (S_i^{rotation}), *i. e.*, $S_i = S_i^{\text{porous}} + S_i^{\text{gravity}} + S_i^{\text{rotation}}$. The thermal enthalpy is h, Q_H – the heat source or sink per unit volume, $\boldsymbol{\tau}_{ik}$ – the viscous shear stress tensor, q_i – the diffusive heat flux. The subscripts are used to denote summation over the three co-ordinate directions.

Governing equations – conjugate

Flow simulation allows predicting simultaneous heat transfer in solid and fluid media with energy exchange between them. Heat transfer in fluids is described by the energy conservation equation where the heat flux is defined by the conservation equation. The phenomenon of anisotropic heat conductivity in solid media is described by the following equation:

$$\frac{\partial \rho e}{\partial t} = \frac{\partial}{\partial x_i}\left(\boldsymbol{\lambda}_i \frac{\partial T}{\partial x_i}\right) + Q_H \tag{5}$$

where e is the specific internal energy, $e = cT$, c – the specific heat, Q_H – the specific heat release (or absorption) per unit volume, and $\boldsymbol{\lambda}_i$ are the eigenvalues of the thermal conductivity tensor. It is supposed that the heat conductivity tensor is diagonal in the considered co-ordinate system. For isotropic medium $\boldsymbol{\lambda}_1 = \boldsymbol{\lambda}_2 = \boldsymbol{\lambda}_3 = \boldsymbol{\lambda}_4$.

Environment and solar radiation models

Environmental and solar radiation can be applied to the internal problems. In fact, the environment radiation is the non-directional energy flux generated by the walls of an imaginary huge *room* that surrounds the body. This flux has predefined radiation parameters. In contrast to the environment radiation, the solar radiation is modeled by the directional energy flux. Therefore, the solar radiation is defined via its power flow (intensity) and its directional vector.

In addition to the solar radiation from the computational domain boundaries, a solar radiation source emitting directional radiation can be specified.

The Sun directional vector can be calculated using the following formula:

$$\vec{S} = [\vec{E}\sin\phi_s + \vec{N}\cos\phi_s]\cos\theta_s + \vec{Z}\sin\theta_s \tag{6}$$

where $\vec{Z}$ is the zenith direction, $\vec{N}$ is the north direction, $\vec{E} = \vec{N}\times\vec{Z}$ is the east direction, and θ_s is the solar elevation angle, *i. e.* the angle between the direction of the geometric center of the Sun's apparent disk and the (idealized) horizon, θ_s is the solar azimuth angle, *i. e.* the angle from due north in a clockwise direction.

The solar elevation angle θ_s can be calculated, to a good approximation, using the following formula [21]:

$$\sin\theta_s = \cos h\cos\delta\cos\phi + \sin\delta\sin\phi \tag{7}$$

where ϕ is the local latitude and δ is the current Sun declination, $h = t/86400(2\pi - \pi)$ is the hour angle of the present time t [s] (for example, at solar noon 12.00 a. m., t = 43200 seconds and h = 0).

Mesh details

Figure 1 shows the mesh details of the computational domain with and without lids and tab. 1 provides the data about the no of fluid, solid and total cells for with and without fin computational domain.

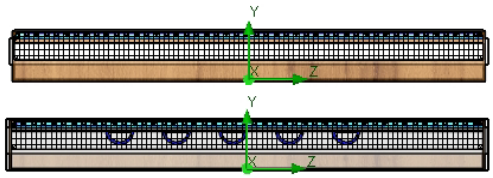

Figure 1. Mesh solid and fluid domain for with and without fins

Table 1. Mesh details for with and without fins

Without fin		With fin	
Total cell count	243948	Total cell count	262406
Fluid cells	107536	Fluid cells	109102
Solid cells	136412	Solid cells	153304
Partial cells	63128	Partial cells	75668

Boundary conditions

Boundary conditions, tab. 2, were taken as mass-flow rate for the inlet and pressure outlet for the outlet of solar air heater, transient solar radiation, and ambient temperature were given as input, as shown in fig. 2, it is a transient analysis done for 7 hours with results time step of every 15 minutes, time step for analysis is 0.01666 seconds, and 20 iterations are given for solving one-time step, a high end computational with 128 GB ram and xenon processor is employed for the analysis of this domain. Turbulence model used for this analysis is *k-ε*. Solid works flow simulations software is used for transient analysis.

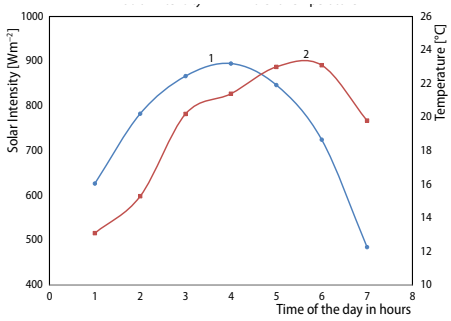

Figure 2. Solar radiation *vs.* ambient temperature boundary condition; *1 – solar intensity, 2 – ambient temperature*

Experimental set-up of solar air heater [22]

A pictorial view of solar air heater is shown in fig. 3, it is a single pass solar air heater in which air-flows between the solar absorber plate and bot-

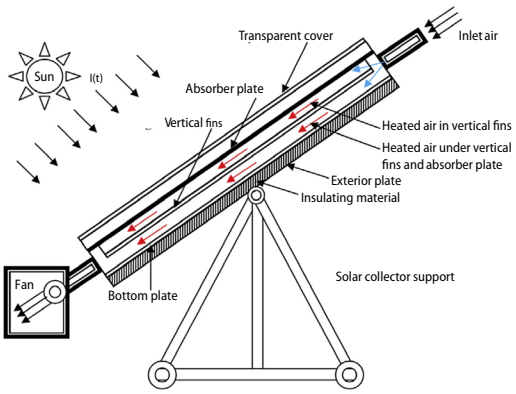

Figure 3. Schematic layout of solar air heater

Table 2. Boundary conditions

Inlet	Mass-flow rate
Outlet	Environment pressure
Solar radiation transient for 7 hours	Refer fig. 1
Time step	0.0166 seconds
Iterations per time step	20

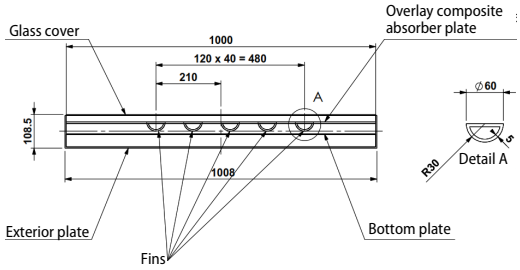

Figure 4. Geometry of solar air heater with and without fins

tom plate, one experiment is made without fins and another with a hollow vertical plate at the bottom of absorber plate as shown in fig. 4. The material for fins and absorber plate are galvanized iron with black chrome coating. The plate thickness of absorber plate is 0.5 mm, glass thickness is 5 mm, thermal insulation expanded polystyrene is given at the surroundings of the heater for 40 mm thickness, solar absorber area is 2 × 1 meter.

Results and discussions

From fig. 5 it is evident that plate temperature decreases by increasing the flow rate, also plate temperature raises by 20% by proving the fins hollow vertical fins at the absorber plates, and temperature rise of 10% increase is seen by varying the flow rate. Figure 6 shows the comparison of experimental versus CFD result for plate temperature, are in good agreement with a maximum error percentage of 11.13%.

Figures 7-10 provides results of inlet temperature and outlet temperature from solar air heater with ambient temperature for four variations which is 0.012 kg/s, 0.016 kg/s with fins

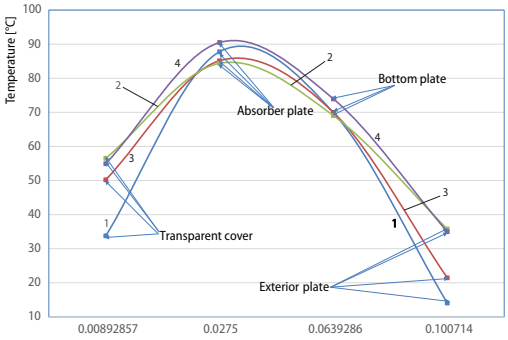

Figure 5. The CFD plate temperatures for 0.012 and 0.016 kg/s with and without fins; *1 – plate temperature without fins 0.012 kg/s, 2 – plate temperature with fins 0.012 kg/s, 3 – plate temperature without fins 0.016 kg/s, and 4 – plate temperature with fins 0.016 kg/s*

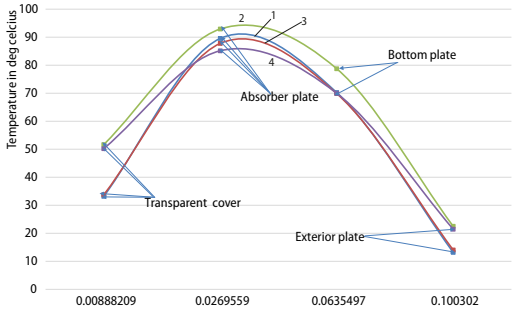

Figure 6. Comparison of experimental *vs.* CFD result for plate temperature; *1 – exp plate tempratures 0.012 kg/s, 2 – exp plate temperatures 0.016 kg/s, 3 – CFD plate temperatures 0.012 kg/s, and 4 – CFD plate temperatures 0.016 kg/s*

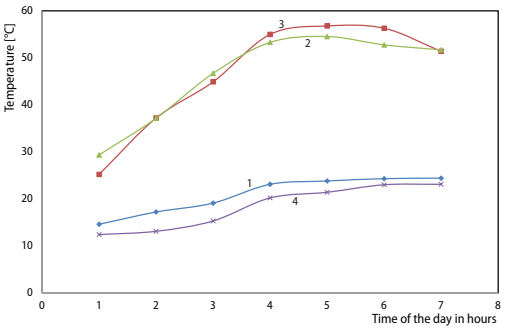

Figure 7. Experimental and CFD outlet temperature with inlet and ambient temperature for without fins at mass-flow rate 0.012 kg/s; *1 – inlet temperature, 2 – outlet temperature CFD, 3 – outlet temperature experimental, and 4 – ambient temperature*

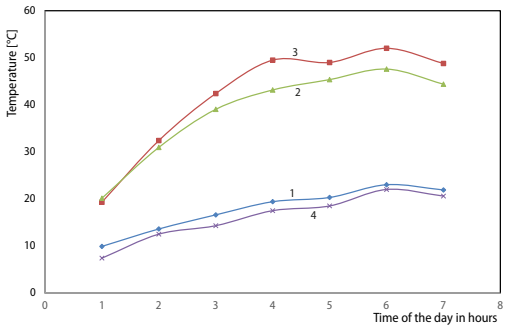

Figure 8. Experimental and CFD outlet temperature with inlet and ambient temperature for without fins at mass-flow rate 0.016 kg/s; *1 – inlet temperature, 2 – outlet temperature CFD, 3 – outlet temperature experimental, and 4 – ambient temperature*

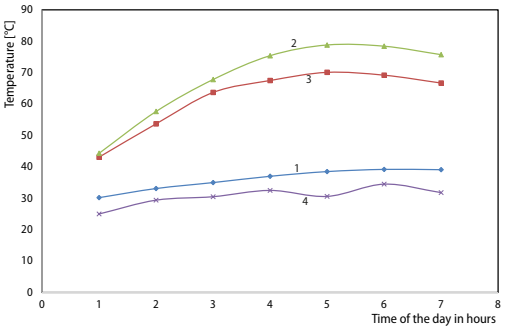

Figure 9. Experimental and CFD temperature outlet with inlet and ambient temperature for with fins at mass-flow rate 0.012 kg/s; *1 – inlet temperature, 2 – outlet temperature CFD, 3 – outlet temperature experimental, and 4 – ambient temperature*

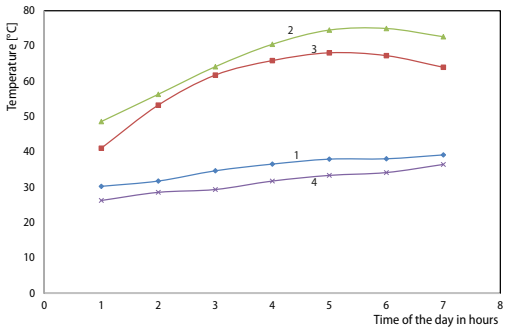

Figure 10. Experimental and CFD outlet temperature with inlet and ambient temperature for with fins at mass-flow rate 0.016 kg/s ; *1 – inlet temperature, 2 – outlet temperature CFD, 3 – outlet temperature experimental, and 4 – ambient temperature*

and without fins, and it is also compared the experimental outlet temperature *vs.* CFD outlet temperature for all the four cases average error percentage between experimental and CFD is 1.7%.

The following observations are made by comparison of the outlet temperature of the air, 25% of improvement in outlet temperature was observed between without fin and with fin configurations, and about 10% of improvement is seen by altering the flow rate from 0.012 to 0.016 kg/s.

Figure 11 shows the CFD outlet temperature comparative chart for four configurations of for two flow rates and with and without fins, in which maximum outlet temperature is achieved by finned configuration of mass-flow rate 0.016 kg/s followed by with fin of 0.012 kg/s, outlet temperature for without fin configuration well below the finned configuration.

Figure 12 shows the velocity plot of without fin configuration for 0.012 and 0.016 kg/s flow rates, velocities per cross section doesn't vary much for two flow rates but for single velocity say 0.35m/s lower flow rate has less coverage in comparison with higher flow rate.

Figure13 shows the velocity plot of with fin configuration for 0.012 and 0.016 kg/s flow rates, where a higher velocity of 0.53 is seen on the inlet, being area is reduced by fins it is velocity increases which also augment the higher heat transfer rate.

Figure 14 shows the transient temperature contour plot for 7 hours without fins, in which max temperature of 55° occurs at 13:00 hours and it sustains for 1 hour, temperature rises to 45 °C by 12:00 and it maintains at 53 °C till 16:00 hours, hence generations a hot air around 45 °C for 4 hours is possible using a solar air dryer without fins with flow rate of 0.016 kg/s.

Figure 15 shows the transient temperature contour plot for 7 hours with fins, in which max temperature of 85° occurs at 14:00 hours and it sustains for 1 hour, temperature rises to 75 °C by 12:00 and it maintains at 80 °C till 16:00 hours, hence generation of hot air around 75 °C for 4 hours is possible using a solar air dryer of hollow verticals fins with flow rate of 0.016 kg/s. by the previous results, it is possible to raise the 30 °C of temperature difference by using the hollow vertical fin configuration.

From figs. 16-19 in which thermal efficiency increases as mass-flow rate increases, thermal efficiency increased from 40% to 51% for mass-flow rates of 0.012 and 0.016 kg/s, respectively, and thermal efficiency increases from 35% to 44% in case of without and with fin configurations.

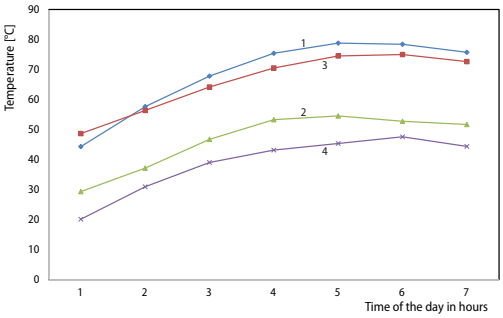

Figure 11. Comparison of outlet temperatures for two flow rate and with and without fin; *1 – CFD outlet tempature for without fins 0.012 kg/s, CFD outlet tempature for with fins 0.012 kg/s, 3 – CFD outlet tempature for without fins 0.016 kg/s, and 4 – CFD outlet tempature for with fins 0.016 kg/s*

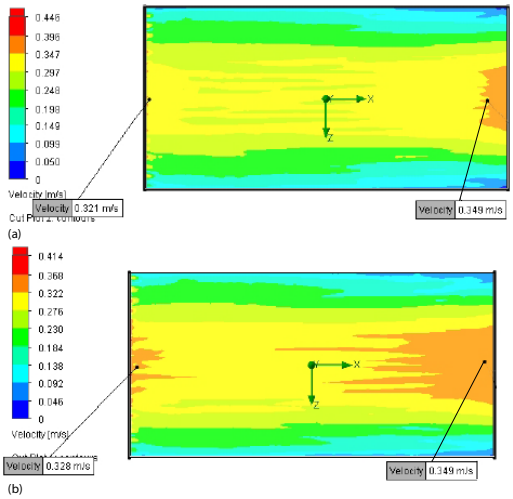

Figure 12. Velocity comparison contour plot for without fin configuration (a) for 0.012 and (b) for 0.016 kg/s (*for color image see journal web site*)

Detailed analysis of results

- Initially, absorber plate temperature decreases by increasing the flow rate, by providing the fins plate temperature increases, experimental plate temperature are in good agreement with CFD plate temperature with an error percentage of 11.13%.
- The outlet temperature of air improves by 25% when observed between without fin and with fin configurations, and about 10% of improvement is seen by altering the flow rate from 0.012 to 0.016 kg/s.
- A hot air around 45 °C for 4 hours is possible using a solar air dryer of without fins with flow rate of 0.016 kg/s whereas a 75 °C of hot air for 4 hours is possible using a solar air dryer of hollow verticals fins
- Thermal efficiency increases as mass-flow rate increases, thermal efficiency increased from 40% to 51% for mass-flow rates of 0.012 and 0.016 kg/s, respectively, and thermal efficiency increases from 35% to 44% in case of without and with fin configurations.

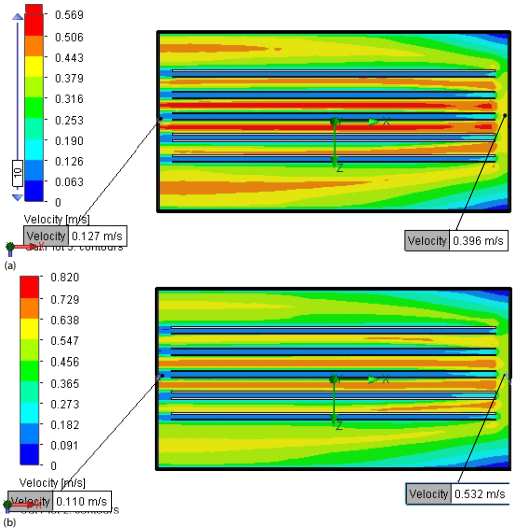

Figure 13. Velocity comparison contour plot for with fin configuration for (a) 0.012 and (b) for 0.016 kg/s (*for color image see journal web site*)

Conclusion

Evaluation of experimental thermal performance of a single pass solar air dryer is compared with a transient CFD studies were performed and the following conclusions are drawn:

- Plate temperature decreases by increasing the flow rate, also plate temperature raises by 20% by proving the fins, and temperature rise of 10% increase is seen by varying the flow rate.
- Experimental *vs.* CFD result for plate temperature is in good agreement with a maximum error percentage of 11.13%.
- Outlet temperature for 4 cases two flow rates, with fin and without fin are in good agreement with experimental results with maximum error percentage 12%

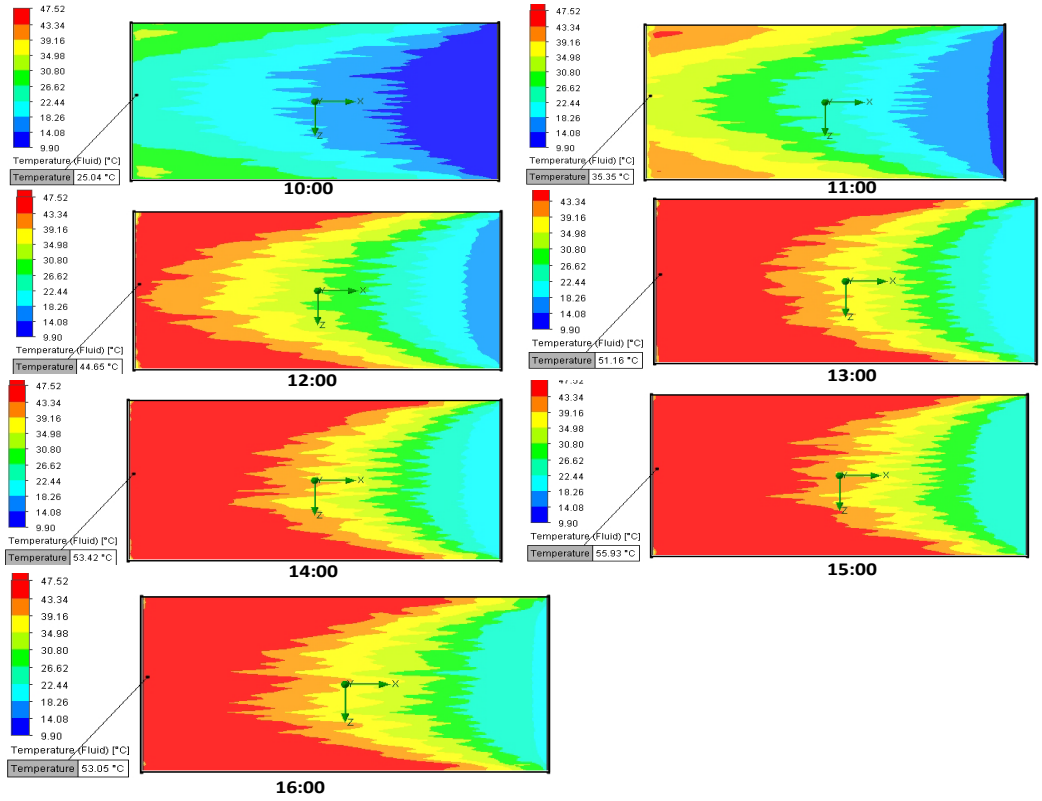

Figure 14. Transient temperature contour plot for 7 hours without fins, 0.016 kg/s (*for color image see journal web site*)

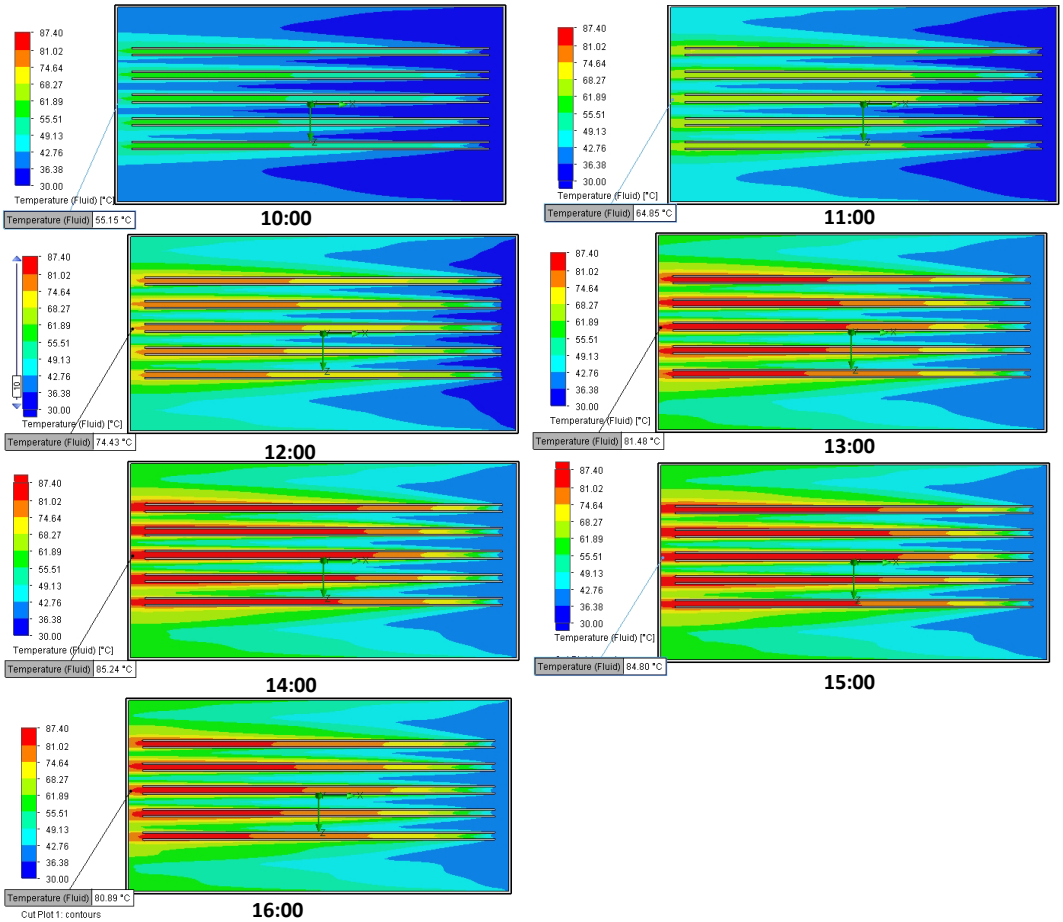

Figure 15. Transient temperature contour plot for 7 hours with fins, 0.016 kg/s
(*for color image see journal web site*)

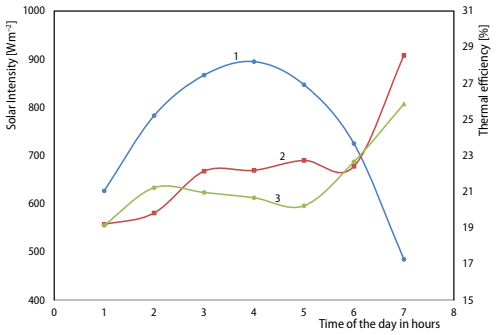

Figure 16. Thermal efficiency *vs.* solar radiation for without fins 0.012 kg/s; *1 – solar intensity, 2 – experimental thermal efficiency, and 3 – CFD thermal efficiency*

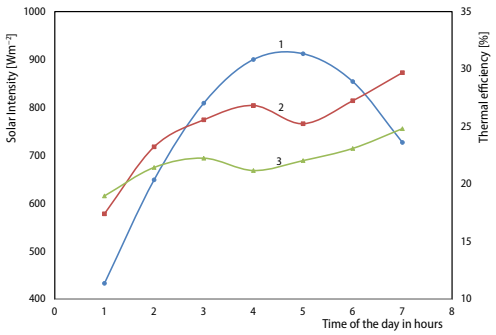

Figure 17. Thermal efficiency *vs.* solar radiation for without fins 0.016 kg/s ; *1 – solar intensity, 2 – experimental thermal efficiency, and 3 – CFD thermal efficiency*

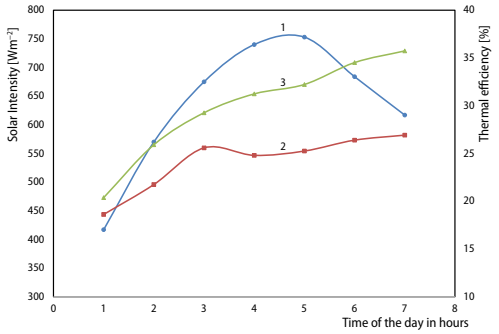

Figure 18. Thermal efficiency *vs.* solar radiation for with fins 0.012 kg/s; *1 – solar intensity, 2 – experimental thermal efficiency, and 3 – CFD thermal efficiency*

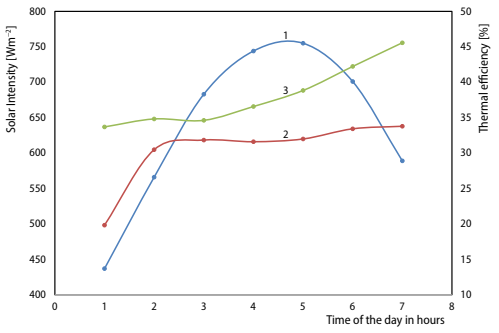

Figure 19. Thermal efficiency *vs.* solar radiation for with fins 0.016 kg/s; *1 – solar intensity, 2 – experimental thermal efficiency, and 3 – CFD thermal efficiency*

- The 25% of improvement in outlet temperature was observed between without fin and with fin configurations, and about 10% of improvement is seen by altering the flow rate from 0.012 to 0.016 kg/s.
- Hot air generation of around 75 °C for 4 hours is possible using a solar air dryer of hollow verticals fins with a flow rate of 0.016 kg/s.
- It is possible to raise 30 °C of temperature difference by using the hollow vertical fin configuration.
- Thermal efficiency is increased from 40% to 51% for mass-flow rates of 0.012 and 0.016 kg/s, respectively, and thermal efficiency increases from 35% to 44% in case of without and with fin configurations.
- To conclude in a general point of view, solar air heater with fins will be beneficial in improving thermal efficiency, generate of hot air for 4 hours at 75 °C

References

[1] Akpinar, E. K., *et al*., Experimental Investigation of the Thermal Performance of Solar Air Heater Having Different Obstacles on Absorber Plates, *International communication on Heat Mass Transfer, 37* (2010), 4, pp. 416-421
[2] Karsli, S., *et al*., Performance Analysis of New-Design Solar Air Collectors for Drying Applications, *Renewable Energy, 32* (2007), 10, pp. 1645-1660
[3] Romdhane, B. S., *et al*., The Air Solar Collectors: Comparative Study, Introduction of Baffles to Favor the Heat Transfer, *Solar Energy, 81* (2007), 1, pp. 139-149
[4] Wenfeng, G., *et al*., Analytical and Experimental Studies on the Thermal Performance of Cross-Corrugated and Flat-Plate Solar Air Heaters, *Applied Energy, 84* (2007), 4, pp. 425-441
[5] Yeh, H. M., *et al*., The Influences of Recycle on Performance of Baffled Double-Pass Flat-Plate Solar Air Heaters with Internal Fins Attached, *Applied Energy, 86* (2009), 9, pp. 1470-1478
[6] EminBilgili, B., *et al*., Experimental Investigation of Three Different Solar Air Heaters: Energy and Exergy Analyses, *Applied Energy, 87* (2010), 10, pp. 2953-2973
[7] Aldabbagh, L. B. Y., *et al*., Experimental Performance of Single and Double Pass Solar Air Heater with Fins and Steel Wire Mesh as Absorber, *Applied Energy, 87* (2010), 12, pp. 3759-3765
[8] Aboul-Enein, S., *et al*., Thermal Performance Investigation of Double Pass-Finned Plate Solar Air Heater, *Applied Energy, 88* (2011), 5, pp. 1727-1739
[9] Singh, D., *et al*., Analysis of a Glass Solar Air Heater, *Energy Conversion mgnt, 23* (1983), 4, pp. 231-236
[10] Ozgen, F., *et al*., Experimental of an Investigation of Thermal Performance Double-Flow Solar Air Heater Having Aluminium Cans, *Renewable Energy, 34* (2009), 11, pp. 2391-2398
[11] Deep Singh, T., *et al*., Performance Evaluation of Solar Air Heater with Novel Hyperbolic Rib Geometry, *Renewable Energy, 105* (2017), May, pp. 786-797

[12] Vipin, B. Gawande., *et al*., Experimental and CFD Investigation of Convection Heat Transfer in Solar Air Heater with Reverse L-Shaped Ribs, *Solar Energy, 131* (2016), June, pp. 275-295
[13] Yadav, A. S., *et al*., A Numerical Investigation of Square Sectioned Transverse Rib Roughened Solar Air Heater, *Int. J. ThermSci., 79* (2014), May, pp.111-131
[14] Aniket Shrikant Ambekar., *et al*., CFD Simulation Study of Shell and Tube Heat Exchangers with Different Baffle Segment Configurations, *Applied Thermal Energy*, *108* (2016), Sept., pp. 999-1007
[15] Debayan, D., *et al*., Role of Distributed/Discrete Solar Heaters during Natural Convection in the Square and Triangular Cavities: CFD and Heatline Simulations, *Solar Energy, 135* (2016), Oct., pp. 130-153
[16] Boulemtafes, B., *et al*., CFD Based Analysis of Heat Transfer Enhancement in Solar Air Heater Provided with Transfer Rectangular Ribs, *Energy Procedia, 50* (2014), Dec., pp. 761-772
[17] Anil Singh Yadav., *et al*., A CFD (Computational Fluid Dynamics) Based Heat Transfer and Fluid Flow Analysis of a Solar Air Heater Provided with Circular Transverse Wire Rib Roughness on the Absorber Plate, *Energy, 55* (2013), June, 1127e1142
[18] Anil Singh Yadav., *et al*., A CFD Based Thermo-Hydraulic Performance Analysis of an Artificially Roughened Solar Air Heater Having Equilateral Triangular Sectioned Rib Roughness on the Absorber Plate, *International Journal of Heat and Mass Transfer, 70* (2014), Mar., pp. 1016-1039
[19] Keguang, Y., Tong, Li., *et al*., Performance Evaluation of All-Glass Evacuated Tube Solar Water Heater with Twist Tape Inserts Using CFD, *Energy Procedia, 70* (2015), May, pp. 332-339
[20] Alsanossi, M., *et al*., Performance Analysis of Solar Air Heater with Jet Impingement on Corrugated Absorber Plates, *Case Studies in Thermal Engineering, 10* (2017), Sept., pp. 111-120
[21] ***, Solid Works Flow Simulations Software, Manual
[22] Foued Chabanea, B., *et al*., Experimental Study of Heat Transfer and Thermal Performance with Longitudinal Fins of Solar Air Heater, *Journal of Advanced Research*, *5* (2013), 2, pp. 1-10

Paper submitted: April 6, 2017
Paper revised: November 2, 2017
Paper accepted: November 5, 2017